Available online at www.sciencedirect.com
ScienceDirect
International Journal of Heat and Mass Transfer 51 (2008) 2905–2913
International Journal of HEAT and MASS TRANSFER
www.elsevier.com/locate/ijhmt

A comprehensive analytical solution of macromolecular transport within an artery

Mehrzad Khakpour, Kambiz Vafai *

Mechanical Engineering Department, University of California, Riverside, CA 92521, USA

Received 7 July 2007; received in revised form 10 September 2007
Available online 13 November 2007

Abstract

Macromolecule transport within an artery is investigated and a comprehensive analytical solution is presented. The transport within the lumen and the arterial wall are coupled. Arterial wall is modeled as a four-layer porous wall. The layers are all treated as macroscopically homogeneous porous media. The volume-averaged porous media equations are employed to solve for transport through the porous arterial layers. Staverman filtration coefficient is incorporated to account for selective permeability of each porous layer to macromolecules. The problem encompasses complex interfacial transport phenomena involving various porous–porous as well as porous–fluid interfaces. The method of matched asymptotic expansions is employed to solve for the fluid flow field and species concentration distributions. For comparison purposes, the physiological and transport parameters associated with each porous layer are obtained from the literature. The analytical results are in excellent agreement with previous numerical studies. The results presented in this work provide the first comprehensive analytical solution representing arterial transport phenomena.

1. Introduction

Cardiovascular diseases (CVD) are the leading causes of death in the United States. The American Heart Association [1] reports that nearly 80 million American adults have one or more types of CVD. Most cardiovascular events are secondary to atherosclerosis, a progressive disorder of the arterial wall. It is characterized by gradual and uneven narrowing of the arteries due to abnormal infiltration and accumulation of macromolecules such as low-density lipoproteins (LDL).

Today, scientists from various fields of study are contributing in achieving a better understanding of the causes, genesis, and development of atherosclerosis through the analysis of the underlying processes. Over the years, various models have been proposed to represent the anatomical structure of the arteries. The models are results of the trade-off between accuracy and feasibility. Khakpour and Vafai [2] have presented a critical assessment of the arterial transport models. As mentioned in their critical review, to date, the multi-layer porous wall model is the most accurate and complex model used in the study of arterial transport phenomena. In this model, the arterial wall is treated as a porous wall composed of four macroscopically homogeneous porous layers. These layers possess different transport properties which dictate the distribution of the macromolecule concentration.

Various analytical, numerical, and experimental/clinical studies have been performed investigating several parameters and processes pertinent to arterial transport. While a great majority of these studies have used numerical and experimental/clinical tools, a few analytical investigations have also been attempted. Although the existing analytical solutions [3] provide useful insight into the arterial transport phenomenon, they are rather simplified, omitting some important aspects. Their major drawback is to reduce the problem to one dimension, neglecting the axial transport. Another shortcoming of the existing analytical

* Corresponding author. Tel.: +1 951 827 2135; fax: +1 951 827 2899.
E-mail address: vafai@engr.ucr.edu (K. Vafai).

0017-9310/$ - see front matter © 2007 Elsevier Ltd. All rights reserved.
doi:10.1016/j.ijheatmasstransfer.2007.09.019

Nomenclature

c	species concentration
D	mass diffusion coefficient
Da	Darcy number
F	dimensionless inertia coefficient
$\vec{J}$	unit vector oriented along the velocity vector
K	permeability
M	non-dimensional concentration
n	direction normal to interface
p	pressure
R	radius of lumen
Re_{ch}	Reynolds number $= (u_{ch}\sqrt{K})/\nu_f$
Sc	Schmidt number
$U_{0,i}$	streamwise velocity at the ith interface
u	streamwise component of velocity field
u_c	Darcian convective velocity
u_{max}	Luminal centerline (maximum) velocity
$\vec{V}$	velocity vector
v	filtration velocity
x	axial location
y	radial location

Greek symbols

ε	gage parameter
ρ	density
δ	porosity
σ_f	Staverman filtration coefficient
μ	dynamic viscosity
ξ	non-dimensional axial location
η	non-dimensional radial location

Subscripts

e	effective property
f	fluid
s	species field
m	momentum field
i	index $i = 0$, 1, 2, 3, and 4 representing lumen, endothelium, intima, IEL, and media, respectively

Symbol

$\langle\rangle$	"local volume average" of a quantity

solutions is to rely on the Kedem–Katchalsky solute transport equation [4], which carries the problem of evaluating the mean solute concentration used in its convective term. As such, there remains a need for a comprehensive analytical solution to the arterial transport phenomena incorporating the axial transport as well as other influential processes. In the present work, a robust theoretical solution to the macromolecule transport within an artery is presented. First, the governing equations are presented. Then the fluid flow and mass transfer analysis is performed at each interface. The method of matched asymptotic expansions along with Laplace transformation is employed to solve for the coupled transport phenomena within lumen and the arterial wall. Using the transport parameters available in the literature, the analytical results are then compared with those obtained via numerical simulations.

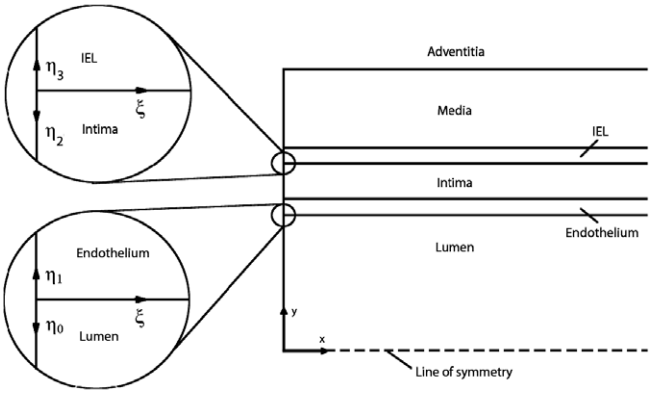

Fig. 1. Schematic illustration of an artery and the coordinate systems used in the analytical solution.

2. Formulation

Steady state blood flow and solute transport within an artery are considered. A schematic of the case of study is presented in Fig. 1. The artery is modeled as a uniform axisymmetric circular pipe with a heterogeneous porous wall. The wall is composed of four different macroscopically homogeneous porous layers: endothelium, intima, internal elastic lamina (IEL), and media. Changes in angular direction are assumed to be negligible; therefore the problem is reduced to two dimensions. Due to symmetry about the x-axis, half of the domain is considered. It should be noted that our presented analytical solution can easily be extended to different models composed of any number of layers making up an arterial wall.

The luminal blood flow is assumed to be Newtonian, isothermal and incompressible. Blood properties (i.e. viscosity and diffusivity) are assumed to be constant. Navier–Stokes equations coupled with mass transport equations (advection–diffusion) are employed to solve for the luminal blood flow and solute transport. These governing equations are given by

$$\nabla \cdot \vec{V} = 0 \tag{1}$$

$$\rho \vec{V} \cdot \nabla \vec{V} = -\nabla p + \mu \nabla^2 \vec{V} \tag{2}$$

$$\vec{V} \cdot \nabla c = D \nabla^2 c \tag{3}$$

where $\vec{V}$ is the velocity vector, p the pressure, ρ the density, μ dynamic viscosity of blood, c the solute concentration, and D is the solute diffusivity within the blood.

Due to complex nature of the arterial transport phenomena, the inertial and boundary effects are to be accounted for. Therefore, the volume-averaged equations of transport through porous media are used to solve for velocity and concentration fields [5,6]. The Staverman filtration coefficient is incorporated to account for selective permeation of species by the membranes [7,8]. The governing equations for the porous layers are given by

$$\nabla \cdot \langle \vec{V} \rangle = 0 \tag{4}$$

$$\frac{\rho_f}{\delta}\langle(\vec{V}\cdot\nabla)\vec{V}\rangle = -\nabla\langle P\rangle^f + \frac{\mu}{\delta}\nabla^2\langle\vec{V}\rangle - \frac{\mu}{K}\langle\vec{V}\rangle - \frac{\rho_f F\delta}{\sqrt{K}}[\langle\vec{V}\rangle\cdot\langle\vec{V}\rangle]\vec{J} \tag{5}$$

$$(1-\sigma_f)\langle\vec{V}\rangle\cdot\nabla\langle c\rangle = D_e\nabla\langle c\rangle^2 + k\langle c\rangle \tag{6}$$

where ρ_f is the fluid density, δ porosity of the porous medium, F dimensionless inertia coefficient, and K is the permeability of the porous medium. The parameters σ_f and D_e represent the Stavernan filtration coefficient and the effective solute diffusivity in the porous medium, respectively. The effective volumetric first-order reaction rate, k, takes a value of zero for endothelium, intima, and IEL. The symbol $\langle\,\rangle$, represents the local volume average of a quantity associated with the fluid. The parameters $\langle P\rangle^f$ and $\vec{J}$ are the average pressure inside the fluid and a unit vector oriented along the velocity vector $\vec{V}$, respectively. It has been shown that the convective term, $\langle(\vec{V}\cdot\nabla)\vec{V}\rangle$, causing boundary layer growth is significant only over a length of the order of $\frac{\rho_f K u_c}{\mu_f}$ where u_c is the Darcian convective velocity. This length is relatively small for most practical situations [6]. Therefore, a fully developed momentum boundary layer is formed over a very short length. For this case, the momentum Eq. (5) reduces to

$$\frac{\mu}{\delta}\nabla^2\langle\vec{V}\rangle - \frac{\mu}{K}\langle\vec{V}\rangle - \frac{\rho_f F\delta}{\sqrt{K}}[\langle\vec{V}\rangle\cdot\langle\vec{V}\rangle]\vec{J} - \nabla\langle P\rangle^f = 0 \tag{7}$$

The blood velocity profile within the lumen is assumed to be laminar and fully developed and is given by

$$u = u_{max}\left(1-(y/R)^2\right) \tag{8}$$

where u_{max} is the centerline (maximum) velocity, R the radius of the lumen, u the streamwise component of the velocity vector, and y is the radial location. A continuity boundary condition is employed at the interface between the layers. This boundary condition requires the value of velocity and its derivative to remain constant across the interface. Similarly, the value of species concentration and the total species flux must remain constant across the interface [9]. At the inlet a uniform and constant species concentration is prescribed. Also, at the media-adventitia interface the concentration gradient in the direction normal to the interface is assumed to be negligible.

In what follows, the method of matched asymptotic expansions is used to solve for the flow field and species concentration distribution. At each step, two media and the interface between them are considered. The coordinate system is chosen to lie at the interface between the two media. It should be noted that several coordinate systems are introduced and used throughout the analysis. A gauge parameter is utilized to non-dimensionalize the coordinate system. The dependent variable of interest (i.e. velocity or species concentration) is expanded in terms of powers of an appropriate parameter. Throughout the analysis, the choice of the gauge parameters involved in the perturbation solutions for velocity and concentration is found to be inherently tied to the physics of the problem and therefore an important physical metric. This leads to the use of a number of different gauge functions for describing the fluid mechanics and the concentration distributions within an artery.

3. Fluid flow analysis

3.1. Fluid flow within lumen and endothelium (fluid–porous)

Lumen, endothelium, and the interface between them are considered. The coordinate system is chosen to lie at the lumen–endothelium interface, as shown in Fig. 1. Solving the Navier–Stokes equation using a slip boundary condition at the interface, the luminal velocity field is found to be

$$u_0 = -\eta_{m,0}^2 + 2\eta_{m,0} + U_{0,1} \tag{9}$$

where $\eta_{m,0} = y_0/R$ is the non-dimensional normal coordinate for the lumen. u_0 and $U_{0,1}$ are the non-dimensionalized streamwise velocities within the lumen and at the lumen–endothelium interface, respectively. The velocity field is non-dimensionalized using a reference velocity given as

$$u_{ch,0} = -\frac{R^2}{2\mu_f}\frac{dp}{dx} \tag{10}$$

It should be noted that at this stage $U_{0,1}$ is unknown. It will be found through evaluation of the velocity field within the endothelium layer, which is governed by Eqs. (4) and (7). By introducing the gauge parameter

$$\varepsilon_{m,1} = \frac{1}{R}\sqrt{\frac{K_1}{\delta_1}} \tag{11}$$

the generalized equation becomes

$$\frac{d^2u_1}{d\eta_{m,1}^2} - u_1 - \alpha_1 u_1^2 + 2\delta_1\varepsilon_{m,1}^2 = 0 \tag{12}$$

where $\eta_{m,1}$ is the non-dimensional normal coordinate for endothelium given by $\eta_{m,1} = y_1/\sqrt{K_1/\delta_1}$. The parameter α_1 is given as $\alpha_1 = F_1\delta_1 Re_{ch,1}$ where $Re_{ch,1} = (u_{ch,0}\sqrt{K_1})/\nu_f$. The non-dimensional streamwise component of velocity vector within the endothelium, $u_1 = \langle u_1\rangle/u_{ch,0}$, is expanded in terms of the powers of the gauge parameter as

$$u_1 = \varepsilon_{m,1}u_{1,1} + \varepsilon_{m,1}^2 u_{1,2} + \varepsilon_{m,1}^3 u_{1,3} \tag{13}$$

Using the method of matched asymptotic expansions, the first three orders of the inner solution for endothelium are found to be

$$u_{1,1} = 2e^{-\eta^*_{m,1}} \tag{14}$$

$$u_{1,2} = -\frac{8\alpha_1}{3}e^{-\eta^*_{m,1}} + \frac{4\alpha_1}{3}e^{-2\eta^*_{m,1}} + 2\delta_1 \tag{15}$$

$$u_{1,3} = \frac{2\alpha_1^2}{3}e^{-3\eta_{m,1}} - \frac{32\alpha_1^2}{9}e^{-2\eta_{m,1}} - 4\alpha_1\delta_1\eta_{m,1}e^{-\eta_{m,1}} + \left(\frac{46\alpha_1^2}{9} - 4\alpha_1\delta_1\right)e^{-\eta_{m,1}} \tag{16}$$

By setting $\eta_{m,1} = 0$, the interface velocity is found to be

$$U_{0,1} = 2\varepsilon_{m,1} + \left(2\delta_1 - \frac{4\alpha_1}{3}\right)\varepsilon^2_{m,1} + \left(\frac{20\alpha_1^2}{9} - 4\alpha_1\delta_1\right)\varepsilon^3_{m,1} \tag{17}$$

Streamwise component of velocity field within the endothelium layer at locations relatively far from the lumen–endothelium interface ($\eta_{m,1} \to \infty$) is given by

$$u_1 = 2\delta_1\varepsilon^2_{m,1} \tag{18}$$

3.2. Fluid flow within the porous arterial layers

A schematic of the coordinate system used in the evaluation of the velocity within intima and IEL is presented in Fig. 1. First, the governing equations are non-dimensionalized using the Darcian convective velocity given as

$$u_{c,i} = -\frac{K_i}{\mu_f}\left(\frac{d\langle p_i\rangle^f}{dx}\right) \tag{19}$$

where the subscript i refers to the properties and parameters of the ith porous medium. The generalized equation of transport through the two porous media (i.e. endothelium and intima) reduces to

$$\frac{d^2u_i}{d\eta^2_{m,i}} - u_i - \alpha_i u_i^2 + 1 = 0 \tag{20}$$

The velocities, u_i, are expanded in terms of powers of porosities, δ_i, as

$$u_i = u_{i,0} + \delta_i u_{i,1} + \delta_i^2 u_{i,2} \tag{21}$$

The solutions for the first three orders of the inner solution for intima are found to be

$$u_{2,0} = 1 + \left(U^0_{0,2} - 1\right)\exp(-\eta_{m,2}) \tag{22}$$

$$u_{2,1} = U^1_{0,2}\exp(-\eta_{m,2}) + \beta_2\begin{pmatrix} -1 + \exp(-\eta_{m,2})\begin{bmatrix} 1 - \eta_{m,2}\left(U^0_{0,2} - 1\right) - \\ 1/3\left(U^0_{0,2} - 1\right)^2 \end{bmatrix} + \\ 1/3\exp(-2\eta_{m,2})\left(U^0_{0,2} - 1\right)^2 \end{pmatrix} \tag{23}$$

$$u_{2,2} = U^2_{0,2}\exp(-\eta_{m,2}) + \beta_2 U^1_{0,2}\begin{pmatrix} -\exp(-\eta_{m,2})\left[\eta_{m,2} + 2/3\left(U^0_{0,2} - 1\right)\right] + \\ 2/3\exp(-2\eta_{m,2})\left(U^0_{0,2} - 1\right) \end{pmatrix} + \beta_i^2\begin{pmatrix} 2 + \exp(-\eta_{m,2})\left[A_2\eta^2_{m,2} + B_2\eta_{m,2} + C_2\right] + \\ \exp(-2\eta_{m,2})[D_2\eta_{m,2} + E_2] + 1/12\exp(-3\eta_{m,2})\left(U^0_{0,2} - 1\right)^3 \end{pmatrix} \tag{24}$$

where

$$A_2 = 1/2\left(U^0_{0,2} - 1\right)^2 \tag{25}$$

$$B_2 = 1/3\left(U^0_{0,2} - 1\right)^2 + 3/2\left(U^0_{0,2} - 1\right) - 1 \tag{26}$$

$$C_2 = 5/36\left(U^0_{0,2} - 1\right)^3 + 2/3\left(U^0_{0,2} - 1\right)^2 - 2/3\left(U^0_{0,2} - 1\right) - 2 \tag{27}$$

$$D_2 = -2/3\left(U^0_{0,2} - 1\right)^2 \tag{28}$$

$$E_2 = 2/3\left(U^0_{0,2} - 1\right)\left[1 - \left(U^0_{0,2} - 1\right) - 1/3\left(U^0_{0,2} - 1\right)^2\right] \tag{29}$$

$$U^0_{0,2} = \frac{1 + \phi_1}{\phi} \tag{30}$$

$$U^1_{0,2} = -\frac{\beta_2}{3\phi}\left[\left(U^0_{0,2}\right)^2\phi_2 + \left(U^0_{0,2}\right)\phi_3 + \phi_4\right] \tag{31}$$

$$U^2_{0,2} = \frac{1}{3\phi}\left[-\beta U^0_{0,2}\left(\phi_3 + 2\phi_2 U^0_{0,2}\right) + \beta_2^2\left(\phi_5\left(U^0_{0,2}\right)^3 + \phi_6\left(U^0_{0,2}\right)^2 + \phi_7 U^0_{0,2} + \phi_8\right)\right] \tag{32}$$

$$\phi = 1 + (r_1/r_2)^{1/2} \tag{33}$$

$$\phi_1 = (r_1/r_2)^{1/2}(r_1r_3)^{-1} \tag{34}$$

$$\phi_2 = 1 + \left(r_4r_2^{3/2}\right)^{-1} \tag{35}$$

$$\phi_3 = 1 + \left(r_1r_4r_3r_2^{3/2}\right)^{-1} \tag{36}$$

$$\phi_4 = 1 + \left(r_1^2r_3^2r_4r_2^{3/2}\right)^{-1} \tag{37}$$

$$\phi_5 = 1 + \left(r_1^{1/2}r_2^{5/2}r_4^2\right)^{-1} \tag{38}$$

$$\phi_6 = 1 + \left(r_1^{3/2}r_2^{5/2}r_3r_4^2\right)^{-1} \tag{39}$$

$$\phi_7 = 1 + \left(r_1^{5/2}r_2^{5/2}r_3^2r_4^2\right)^{-1} \tag{40}$$

$$\phi_8 = 1 + \left(r_1^{7/2}r_2^{5/2}r_3^3r_4^2\right)^{-1} \tag{41}$$

$$r_1 = \frac{K_1}{K_2} \tag{42}$$

$$r_2 = \frac{\delta_1}{\delta_2} \tag{43}$$

$$r_3 = \frac{(dp/dx)_1}{(dp/dx)_2} = 1 \tag{44}$$

$$r_4 = \frac{F_1}{F_2} \tag{45}$$

A similar approach is used to obtain the velocity distribution within the IEL and Media layers. The dimensional values of the streamwise component of the velocity field for each layer relatively far from the interfaces ($\eta_{m,i} \to \infty$) are given as

$$u_{1,\infty} = 2\delta_1 \varepsilon_{m,1}^2 u_{ch,0} \tag{46}$$

$$u_{2,\infty} = \frac{K_2}{K_1}\left(2\delta_1 \varepsilon_{m,1}^2 u_{ch,0}\right)\left(1 - \alpha_2 + 2\alpha_2^2\right) \tag{47}$$

$$u_{3,\infty} = \frac{K_3}{K_1}\left(2\delta_1 \varepsilon_{m,1}^2 u_{ch,0}\right)\left(1 - \alpha_3 + 2\alpha_3^2\right) \tag{48}$$

$$u_{4,\infty} = \frac{K_4}{K_1}\left(2\delta_1 \varepsilon_{m,1}^2 u_{ch,0}\right)\left(1 - \alpha_4 + 2\alpha_4^2\right) \tag{49}$$

Darcy's law is employed to calculate the filtration velocity across the arterial wall (in a direction normal to the luminal blood flow). Applying Darcy's law to the arterial wall and observing the continuity of the filtration velocity across the arterial layers, we get

$$v = -\frac{K_{wall}}{\mu_f}\left.\frac{\Delta p}{l}\right|_{wall} \tag{50}$$

where v is the filtration velocity, $\left.\frac{\Delta p}{l}\right|_{wall}$ is the transmural pressure gradient, and K_{wall} is the average permeability of the arterial wall given by

$$\left.\frac{l}{K}\right|_{wall} = \sum_i \frac{l_i}{K_i} \tag{51}$$

where the index i represents the arterial layers.

4. Mass transfer analysis

In this section, analytical solutions are obtained for concentration distributions within the arterial wall. The governing species conservation equation was earlier presented in its general form as Eqs. (3) and (6). The method of matched asymptotic expansions is used to solve for the concentration profiles. In non-dimensional form the species concentration equation is given by

$$u\frac{\partial M}{\partial \xi} + v\frac{\partial M}{\partial \eta_s} = D_e \frac{\partial^2 M}{\partial \eta_s^2} \tag{52}$$

where u and v are the non-dimensional components of the velocity vector given by

$$u = (1 - \delta_f)\langle u\rangle / u_{ch} \tag{53}$$

$$v = (1 - \delta_f)\langle v\rangle / u_{ch} \tag{54}$$

and M represents the non-dimensional species concentration.

4.1. Mass transport at the lumen–endothelium interface

In this part, lumen, endothelium, and the interface between them are considered. The chosen coordinate system is shown in Fig. 1. In the vicinity of the lumen–endothelium interface, it is assumed that the radial component of the velocity vector within the lumen remains constant and equal to the filtration velocity. Inside the concentration boundary layer, we are interested in small values of η_m. This suggests expansions of the streamwise component of the velocity vector for small values of η_m. This results in

$$u_0 = U_0 + 2\eta_{s,0} Sc_0^{-1/2}\sqrt{K/R^2} \tag{55}$$

$$U_{0,1} = 2\varepsilon_{m,1} + \left(2\delta_1 - \frac{4\alpha_1}{3}\right)\varepsilon_{m,1}^2 + \left(\frac{20\alpha_1^2}{9} - 4\alpha_1\delta_1\right)\varepsilon_{m,1}^3 \tag{56}$$

$$u_1 = \left(2 - \eta_{s,1} Sc_1^{-1/2}\right)\varepsilon_{m,1} + \left(2\delta_1 - \frac{4\alpha_1}{3}\right)\varepsilon_{m,1}^2 + \left(\frac{20\alpha_1^2}{9} - 4\alpha_1\delta_1\right)\varepsilon_{m,1}^3 \tag{57}$$

where $\eta_{s,0}$ and $\eta_{s,1}$ are non-dimensional coordinates used in the mass transfer analysis and are given by

$$\eta_{s,0} = y_0/\varepsilon_{s,0} = y_0\sqrt{\frac{Sc_0}{K}} \tag{58}$$

$$\eta_{s,1} = y_1/\varepsilon_{s,1} = y_1\sqrt{\frac{\delta Sc_1}{K}} \tag{59}$$

where Sc is the Schmidt number. Using the coordinate transformation and the velocity distribution given in Eqs. (55)–(57), the species conservation equation and the corresponding boundary conditions for lumen can be written as

$$-V\frac{\partial M_0}{\partial \eta_{s,0}} + \left[U_{0,1} + 2\eta_{s,0} Sc_0^{-1/2}\sqrt{K/R^2}\right]\frac{\partial M_0}{\partial \xi} = \frac{1}{Re_{ch,0}\sqrt{Da_1}}\frac{\partial^2 M_0}{\partial \eta_{s,0}^2} \tag{60}$$

$$M_0(\xi = 0, \eta_{s,0}) = 0 \tag{61}$$

$$M_0(\xi, \eta_{s,0} = 0) = f_0(\xi) \tag{62}$$

Similarly, for the endothelium, the equation can be written as

$$V\frac{\partial M_1}{\partial \eta_{s,1}} + \left[U_{0,1} - \eta_{s,1} Sc_1^{-1/2}\varepsilon_{m,1}\right]\frac{\partial M_1}{\partial \xi} = \frac{1}{Re_{ch,1}\sqrt{Da_1}}\frac{\partial^2 M_1}{\partial \eta_{s,1}^2} \tag{63}$$

$$M_1(\xi = 0, \eta_{s,1}) = 0 \tag{64}$$

$$M_1(\xi, \eta_{s,1} = 0) = f_1(\xi) \tag{65}$$

where the non-dimensional concentrations are given by

$$M_i = \frac{c_i - c_{\infty,i}}{c_{ref}} \tag{66}$$

The concentration field is expanded in terms of $Sc^{-1/2}$ as

$$M_i(\xi, \eta_{s,i}) = M_i^1(\xi, \eta_{s,i}) + M_i^2(\xi, \eta_{s,i})Sc_i^{-1/2} + \cdots \tag{67}$$

with the interface concentration expanded as

$$f_i(\xi, \eta_{s,i}) = f_i^1(\xi, \eta_{s,i}) + f_i^2(\xi, \eta_{s,i})Sc_i^{-1/2} + \cdots \tag{68}$$

As mentioned before, the interface concentration itself is obtained using the continuity conditions for both mass concentration and flux. Using the method of matched asymptotic expansions and Laplace transformations, the zeroth- and first-order luminal concentration distributions are found to be

$$M_0^0(\xi,\eta_{s,0}) = f_0^0 \exp(-A_0)\left[\left(1+\frac{B_0^2C_0}{2}\right)Erfc\left(\frac{B_0}{2\sqrt{\xi}}\right) - \frac{B_0C_0}{\sqrt{\pi}}\sqrt{\xi}\exp\left(-\frac{B_0^2}{4\xi}\right)\right] \quad (69)$$

$$M_0^1(\xi,\eta_{s,0}) = \frac{f_0^1\exp(-A_0)}{8}\left[(8+2B_0^2C_0)\sqrt{\xi}\exp\left(-\frac{B_0^2}{4\xi}\right) - B_0\sqrt{\pi}(4+B_0^2C_0+2C_0\xi)Erfc\left(\frac{B_0}{2\sqrt{\xi}}\right)\right] + \frac{f_0^0\theta_0\exp(-A_0-C_0\xi)\eta_{s,0}^3}{4\sqrt{\pi}B_0^2\sqrt{\xi}}\left[B_0\exp\left(-\frac{B_0^2}{4\xi}\right) - Erfc\left(\frac{B_0}{2\sqrt{\xi}}\right)\right] \quad (70)$$

It should be noted that the presented luminal concentration distribution applies to close proximities of the lumen–endothelium interface, where the normal component of velocity is assumed constant and equal to the filtration velocity across the wall. The zeroth and first order concentration distributions within endothelium are found to be

$$M_1^0(\xi,\eta_{s,1}) = f_1^0\exp(A_1)\left[\left(1+\frac{B_1^2C_1}{2}\right)Erfc\left(\frac{B_1}{2\sqrt{\xi}}\right) - \frac{B_1C_1}{\sqrt{\pi}}\sqrt{\xi}\exp\left(-\frac{B_1^2}{4\xi}\right)\right] \quad (71)$$

$$M_1^1(\xi,\eta_{s,1}) = \frac{f_1^1\exp(A_1)}{8}\left[(8+2B_1^2C_1)\sqrt{\xi}\exp\left(-\frac{B_1^2}{4\xi}\right) - B_1\sqrt{\pi}(4+B_1^2C_1+2C_1\xi)Erfc\left(\frac{B_1}{2\sqrt{\xi}}\right)\right] + \frac{f_1^0\theta_1\exp(A_1-C_1\xi)\eta_{s,1}^3}{4\sqrt{\pi}B_1^2\sqrt{\xi}}\left[B_1\exp\left(-\frac{B_1^2}{4\xi}\right) - Erfc\left(\frac{B_1}{2\sqrt{\xi}}\right)\right] \quad (72)$$

We have

$$A_i = \frac{V\eta_{s,i}}{2Q_i} \quad (73)$$

$$B_i = \eta_{s,i}\sqrt{U_{0,1}/Q_i} \quad (74)$$

$$C_i = \frac{V^2}{4U_{0,1}Q_i} \quad (75)$$

$$Q_i = \frac{1}{Re_{ch,i}\sqrt{Da_i}} \quad (76)$$

$$\theta_0 = \frac{2\sqrt{K}}{R} \quad (77)$$

$$\theta_1 = -\varepsilon_{m,1} \quad (78)$$

where index i takes the values $i=0$, 1 representing lumen and endothelium, respectively.

4.2. Species transport within intima and IEL

Consider endothelium and intima and the interface between them. Using the coordinate system presented in Fig. 1, the species conservation equation can be written as

$$V_i\frac{\partial M_i}{\partial\eta_{s,i}} + \left[U_{0,2}+\Lambda_i\eta_{s,i}Sc_i^{-1/2}\right]\frac{\partial M_i}{\partial\xi} = \frac{1}{Re_{ch,i}\sqrt{Da_i}}\frac{\partial^2 M_i}{\partial\eta_{s,i}^2} \quad (79)$$

where index i takes the values of $i=1$, 2 representing endothelium and intima, respectively. $U_{0,2}$ represents the streamwise component of velocity field at the interface between the two media. According to the coordinate system presented in Fig. 1, the filtration velocity takes different signs within endothelium and intima, i.e. $V_2 = V$ and $V_1 = -V$. Also, the parameter Λ_i is given by

$$\Lambda_i = \left(1-U_{0,i}^0\right) - \delta_i\left[U_{0,i}^1 + \frac{\beta_1}{3}\left(\left(U_{0,i}^0\right)^2 + U_{0,i}^0 + 1\right)\right] - \delta_i^2\left[U_{0,i}^2 + \frac{\beta_1U_{0,i}^1}{3}\left(2U_{0,i}^0+1\right) + \frac{\beta_1^2U_{0,i}^1}{18}\left(7\left(U_{0,i}^0\right)^3 - 11\left(U_{0,i}^0\right)^2 - 62U_{0,i}^0 + 72\right)\right] \quad (80)$$

The normal coordinates are defined as

$$\eta_{s,i} = y_i/\varepsilon_{s,i} = y_i\sqrt{\frac{Sc_i\delta_i}{K_i}} \quad (81)$$

The concentration field is expanded similar to Eqs. (67) and (68). Using the method of matched expansions, Laplace transforms in ξ domain, and the continuity of species concentration and flux at the interface, the zeroth- and first-order concentration distributions in the intima are found to be

$$M_i^0(\xi,\eta_{s,i}) = f_i^0\exp(A_i)\left[\left(1+\frac{B_i^2C_i}{2}\right)Erfc\left(\frac{B_i}{2\sqrt{\xi}}\right) - \frac{B_iC_i}{\sqrt{\pi}}\sqrt{\xi}\exp\left(-\frac{B_i^2}{4\xi}\right)\right] \quad (82)$$

$$M_i^1(\xi,\eta_{s,i}) = \frac{f_i^1\exp(A_i)}{8}\left[(8+2B_i^2C_i)\sqrt{\xi}\exp\left(-\frac{B_i^2}{4\xi}\right) - B_i\sqrt{\pi}(4+B_i^2C_i+2C_i\xi)Erfc\left(\frac{B_i}{2\sqrt{\xi}}\right)\right] + \frac{f_i^0\Lambda_i\eta_{s,i}^3}{4\sqrt{\pi}B_i^2\sqrt{\xi}}\exp(A_i-C_i\xi)\left[B_i\exp\left(-\frac{B_i^2}{4\xi}\right) - Erfc\left(\frac{B_i}{2\sqrt{\xi}}\right)\right] \quad (83)$$

where

$$A_i = \frac{V_i\eta_{s,i}}{2Q_i} \quad (84)$$

$$B_i = \eta_{s,i}\sqrt{U_{0,2}/Q_i} \quad (85)$$

$$C_i = \frac{V_i^2}{4U_{0,2}Q_i} \quad (86)$$

A similar approach can also be used to find the species concentration profile within IEL.

4.3. Species transport within media

Consider IEL and media and the interface between them. The species conservation equation for IEL can be written as

$$-V\frac{\partial M_3}{\partial \eta_{s,3}}+\left[U_{0,4}+\Lambda_3\eta_{s,3}Sc_3^{-1/2}\right]\frac{\partial M_3}{\partial \xi}=\frac{1}{Re_{ch,3}\sqrt{Da_3}}\frac{\partial^2 M_3}{\partial \eta_{s,3}^2} \tag{87}$$

In the case of LDL transport, a chemical reaction occurs within media. This reaction process is modeled as an irreversible first-order chemical reaction. The species conservation equation within the media layer is given by

$$V\frac{\partial M_4}{\partial \eta_{s,4}}+\left[U_{0,4}+\Lambda_4\eta_{s,4}Sc_4^{-1/2}\right]\frac{\partial M_4}{\partial \xi}=\frac{1}{Re_{ch,4}\sqrt{Da_4}}\frac{\partial^2 M_4}{\partial \eta_{s,4}^2}-r_c M_4-R_c \tag{88}$$

where r_c is the non-dimensional chemical reaction rate given as

$$r_c=\frac{k\varepsilon_{s,4}}{u_{ch,0}} \tag{89}$$

The term R_c is the residue of the non-dimensionalization process of the chemical reaction term and is given by

$$R_c=\frac{kc_{\infty,4}\varepsilon_{s,4}}{u_{ch,0}c_{ref}} \tag{90}$$

Index i takes the values of $i=3$, 4 representing IEL and media, respectively. Using the method of matched asymptotic expansions, Laplace transform in ξ domain, and the continuity of species concentration and flux at the interface, the zeroth- and first-order concentration distributions in the intima are found to be

$$\begin{aligned}M_4^0(\xi,\eta_{s,4})=&\left(f_4^0+\frac{R_c}{r_c}\right)\exp(A_4)\left[\left(1+\frac{B_4^2C_4}{2}\right)Erfc\left(\frac{B_4}{2\sqrt{\xi}}\right)-\frac{B_4C_4}{\sqrt{\pi}}\sqrt{\xi}\exp\left(-\frac{B_4^2}{4\xi}\right)\right]\\&-\frac{R_c}{r_c}\exp(A_4-G\xi)\left[\left(1+\frac{B_4^2(C_4-G)}{2}\right)\times Erfc\left(\frac{B_4}{2\sqrt{\xi}}\right)-\frac{B_4(C_4-G)}{\sqrt{\pi}}\sqrt{\xi}\exp\left(-\frac{B_4^2}{4\xi}\right)\right]\\&-\frac{R_c}{r_c}[1-\exp(-G\xi)]\end{aligned} \tag{91}$$

$$\begin{aligned}M_4^1(\xi,\eta_{s,4})=&\frac{f_4^1\exp(A_4)}{8}\left[\left(8+2B_4^2C_4\right)\sqrt{\xi}\exp\left(-\frac{B_4^2}{4\xi}\right)-B_4\sqrt{\pi}(4+B_4^2C_4+2C_4\xi)Erfc\left(\frac{B_4}{2\sqrt{\xi}}\right)\right]\\&+\frac{\left(f_4^0+\frac{R_c}{r_c}\right)\theta_4\exp(A_4-C_4\xi)\eta_{s,4}^3}{4\sqrt{\pi}B_4^2\sqrt{\xi}}\\&\times\left[B_4\exp\left(-\frac{B_4^2}{4\xi}\right)-Erfc\left(\frac{B_4}{2\sqrt{\xi}}\right)\right]\end{aligned} \tag{92}$$

$$A_4=\frac{V_4\eta_{s,4}}{2Q_4} \tag{93}$$

$$B_4=\eta_{s,4}\sqrt{U_{0,4}/Q_4} \tag{94}$$

$$C_4=\frac{V_4^2+4r_cQ_4}{4U_{0,4}Q_4} \tag{95}$$

$$G=\frac{r_c}{U_{0,4}} \tag{96}$$

5. Results and discussion

In this section, the derived analytical results are compared with previously obtained numerical results utilizing the transport properties pertinent to LDL transport. The transport and physiological properties are taken from literature [7] and presented in Table 1. The results are discussed for different pertinent parameters.

5.1. Velocity field

Using Eq. (51), the average arterial permeability is found to be $K_{wall}=3.77\times10^{-19}$ m^2. Subsequently, the filtration velocity for transmural pressures of 70 mm Hg and 160 mm Hg is calculated to be 2.283×10^{-8} m/s and 5.218×10^{-8} m/s, respectively. These values are within roughly 1% of the ones reported by Yang and Vafai [7].

The radial variation of the streamwise component of the velocity field, u, is calculated using Eqs. (22)–(49). Unlike the filtration velocity, the streamwise velocity is different in each layer, with endothelium and intima having the lowest and highest values, respectively. Streamwise velocity within endothelium is roughly four orders of magnitude smaller than that within intima. Therefore, neglecting the streamwise velocity and its convective effects may be justified for endothelium but it can result in significant error in intimal mass concentration distribution.

Table 1
Physiological properties of the arterial layers

	Endothelium	Intima	IEL	Media
Thickness, l (m)	2×10^{-6}	1×10^{-5}	2×10^{-6}	2×10^{-4}
Permeability, K (m^2)	4.32×10^{-21}	2.00×10^{-16}	4.392×10^{-19}	2.00×10^{-18}
Porosity, δ	0.0005	0.983	0.002	0.258
Effective diffusivity, D_e (m^2/s)	6.00×10^{-17}	5.40×10^{-12}	3.18×10^{-15}	5.00×10^{-14}
Filtration reflection coefficient, σ_f	0.9979	0.8272	0.9827	0.8836
Reaction rate coefficient, r (1/s)	0.00	0.00	0.00	3.197×10^{-4}

5.2. LDL transport

Fig. 2 shows the radial variation of LDL concentration across intima and IEL layers for different values of transmural pressure and endothelium effective diffusivity at an axial location of $x = 60$ mm. The results are in good agreement (within 1%) with the numerical results of Yang and Vafai [7]. Fig. 3 shows the variation of LDL concentration within media layer for different values of transmural pressure and endothelium effective diffusivity at an axial location of $x = 60$ mm. The analytical results predict a slightly faster decay in LDL concentration within media. Overall, there exists a good agreement between the numerical and analytical results. Radial variation of LDL concentration across intima and IEL layers at different axial locations are presented in Fig. 4. These results correspond to a transmural pressure of $\Delta P = 160$ mm Hg and endothelium effective diffusivity of $D_e = 2.40 \times 10^{-16}$. The axial variation of LDL concentration predicted by the analytical solution is in excellent agreement with the numerical results.

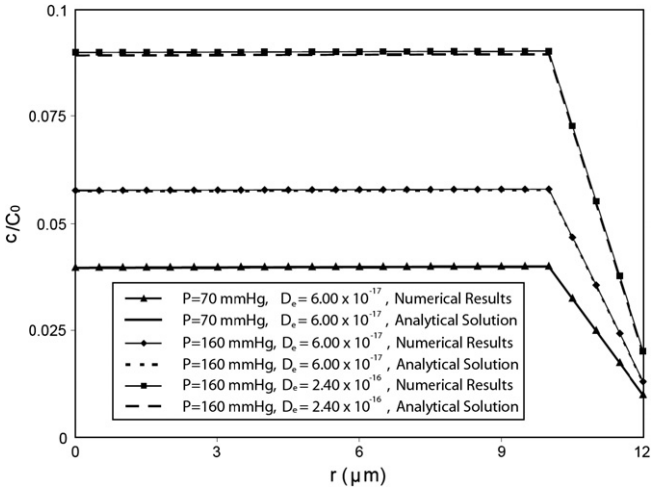

Fig. 2. Radial variation of LDL concentration across intima and IEL layers (radial distance with respect to endothelium–intima interface) for different values of transmural pressure and endothelium effective diffusivity, $x = 60$ mm.

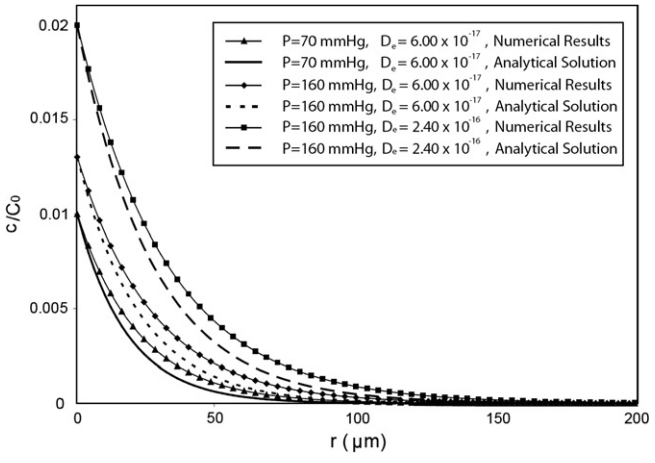

Fig. 3. Variation of LDL concentration within media (radial distance with respect to IEL-media interface) for different values of transmural pressure and endothelium effective diffusivity, $x = 60$ mm.

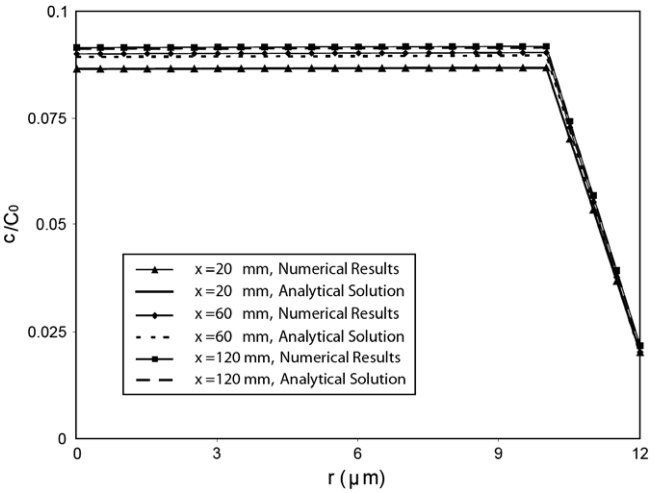

Fig. 4. Radial variation of LDL concentration across intima IEL layers (radial distance with respect to endothelium–intima interface) at different axial locations.

6. Conclusions

Arterial transport is analyzed and a comprehensive analytical solution for the fluid flow and macromolecule transport within an artery is presented. The artery is modeled as a uniform axisymmetric circular pipe with a heterogeneous porous wall. The wall is composed of four different macroscopically homogeneous porous layers. Changes in angular direction are assumed to be negligible; therefore the problem is reduced to two dimensions. Due to symmetry, we only consider half the arterial section. Navier–Stokes equations coupled with mass transport equations are employed to solve for the luminal blood flow and solute transport. The volume-averaged equations of transport through porous media are used to solve for velocity and concentration fields. The Staverman filtration coefficient is incorporated to account for selective permeation of species by the membranes. The method of matched asymptotic expansions in conjunction with Laplace transformation is used to solve for the flow field and species concentration distribution. The analytical solutions are found to be in excellent agreement with the numerical results. The results presented in this work provide the very first comprehensive analytical solution representing arterial transport phenomena. Our analytical solution can easily be extended to different models composed of any number of layers making up an arterial wall.

References

[1] American Heart Association Heart Disease and Stroke Statistics-2007 Update. American Heart Association, Dallas, TX, 2007.

[2] M. Khakpour, K. Vafai, Critical assessment of arterial transport models, Int. J. Heat Mass Transfer (2007), doi:10.1016/j.ijheatmasstransfer.2007.04.021.
[3] N. Yang, K. Vafai, low-density lipoprotein (LDL) transport in an artery – a simplified analytical solution, Int. J. Heat Mass Transfer (2007), doi:10.1016/j.ijheatmasstransfer.2007.05.023.
[4] O. Kedem, A. Katchalsky, Thermodynamic analysis of the permeability of biological membranes to non-electrolytes, Biochim. Biophys. Acta 27 (1958) 229–246.
[5] K. Vafai, C.L. Tien, Boundary and inertia effects on convective mass transfer in porous media, Int. J. Heat Mass Transfer 25 (1982) 1183–1190.
[6] K. Vafai, C.L. Tien, Boundary and inertia effects on flow and heat transfer in porous media, Int. J. Heat Mass Transfer 24 (1981) 195–203.
[7] N. Yang, K. Vafai, Modeling of low-density lipoprotein (LDL) transport in the artery – effects of hypertension, Int. J. Heat Mass Transfer 49 (2006) 850–867.
[8] L. Ai, K. Vafai, A coupling model for macromolecule transport in a stenosed arterial wall, Int. J. Heat Mass Transfer 49 (2006) 1568–1591.
[9] K. Vafai, R. Thiyagaraja, Analysis of flow and heat transfer at the interface region of a porous medium, Int. J. Heat Mass Transfer 30 (1987) 1391–1405.